Quasi-stationary Stefan problem and computer simulation of interface dynamics.

R. Andrushkiw, V. Gafiychuk, and R. Zabrodsky

ABSTRACT. The computer simulation of quasistationary Stefan problem has been realized. Different representations of the Laplacian growth model are considered. The main attention has been paid for the interface dynamics represented by integro differential equations. Numerical approach has been realized by use of interpolating polynomials and exact quadrature formulae. As a result system of ordinary differential equations has been simulated.

There are various physical processes in nature, such as crystallization, combustion, deposition etc., which make it is possible to single out moving boundary having physical properties different on its either side. The location of the given boundary is not known beforehand and is determined self-consistently by the distribution of its physical parameters in the ambient space. Such problems as usually are singled out as a separate section of modern mathematical physics, where the problems with the moving boundaries, also known as Stefan problems, are considered. The number of publications, devoted to this problem, is rather great. Therefore, we will mention only some monographs [1, 2] including a lot of bibliographies on mathematical models of various physical systems containing moving boundaries.

Such problems, as usual, have no analytical solution due to the essential non-linearity stipulated by representation of boundary conditions for selfconsistent parameters allocated on the free boundary. Though it is sometimes possible to find an analytically self-similar solution to a Stefan problem in one-dimensional or quasi-one-dimensional case, concerning the two-dimensional case such problems can be solved using computer simulation only. Due to the fact that problems with the moving boundaries describe a wide class of important technological processes, such as crystallization, melting, etching, oxidation, deposition, diffusion etc., development of numerical methods of their solution is especially important [1, 2].

1. Model

Let us consider crystallization of an undercooled melt located in infinite container, with initial temperature $T < T_c$, where T_c is the temperature of crystallization [3]. It is supposed that growth of the interface of the solid and liquid phases Γ is controlled by the extract of heat generated in the process of crystallization inside the melt (Fig. 1). Then the velocity v_n of the motion of the crystallization front along the normal vector \mathbf{n} to the interface Γ is given by the expression:

Key words and phrases. Laplacian growth, free boundary, dissipative structures, instability.

1

FIGURE 1. A schematic view of the interface during crystallization.

$$(1.1) v_n = -\frac{\varkappa}{\rho L} (\nabla T|_{\Gamma} \mathbf{n}).$$

In the melt the distribution of temperature T is determined by the heat equation:

$$(1.2) c_{\rho}\rho \frac{\partial T}{\partial t} = \varkappa \triangle T.$$

Here c_{ρ} and ρ are the specific heat and density of the liquid phase; \varkappa is thermal conductivity; L is the latent heat of crystallization. The temperature T_s at the crystallization front usually satisfies the Gibbs-Thomson condition:

$$(1.3) T_s = T_c(1 - Kd_0),$$

where K is the local curvature of the surface; d_0 is the capillary length proportional to the surface energy.

It is known that in systems described by equations (1.1) - (1.3) regular dynamics of the interface is unstable. The basic issues for understanding the processes of dissipative structures formation during crystallization are presented in [4, 5], clarifying the reason of formation of these structures for instance the morphological instability. In case of the undercooled melt the mechanism of this instability is stipulated by magnification of the motion velocity of convex segments of the surface penetrating into the undercooled region. The latter stimulates their faster propagating into depth of the melt.

The realization of instability of the homogeneous state of an interface for crystallization of the undercooled melt, within a wide interval of wave numbers and the essential instability of the whole process of shaping, reduces itself to large varieties of possible structures and next to the reproduction of the self-similar forms of the interface in smaller scales. It also indicates the fractal character of their formation. In spite of apparent simplicity of the problem statement, even in two-dimensional domains it is often senseless to perform direct numerical calculations for solving the problem

In same cases the microscopic temporal scales of the parameters specifying the problem changes can appear to be considerably smaller than the temporal scales of dissipation and distribution of an appropriate unlocal field. As a result the distribution of the unlocal field can be considered quasistationary subject to the

location of the boundary. In this case one can construct the equations of surface motion containing only undefined fields specified on the considered surface. It is the basic methodology for this approach.

The essence of the method devised in [3, 6] implies replacement of a consistent system of equations of motion by means of more simple ones, while keeping all the properties of the origin problem. As the velocity in the obtained equations is defined locally at each point, we obtain a set of equations of local dynamics. Some simplifications, however, restricted application of the approach proposed. We can see that the equations obtained in [3] are satisfied for undercooling, when the characteristic scale of an unlocal field (for example temperature) $l_t = \varkappa (c\rho v)^{-1}$ is much smaller than the radius of surface curvature, r i.e.: $l_t \ll r$. Although in this case one can not obtain solutions without numerical simulation making use of appropriate approximations allows to find new solutions, for example those in the form similar to snowflake.

If $l_t \gg r$, then in the field of spatial changes of the temperature it is possible to allocate two characteristic subregions. The first one, with characteristic scale, comparable to l_t , corresponds to the change of the temperature, due to the effect of thermal conduction, when the curvature of the boundary element can be neglected. The second subregion lies in proximity to the boundary element, and its thickness is equal to the average curvature radius r. The change of the temperature and its gradient in this subregion depends on curvature of the boundary. The modulation of the surface temperature and its spatial distribution, as the first approximation in the parameter r/l_t , corresponds to the Laplace equation. Since harmonic functions as the solution of Laplace equation describing the distribution of temperature, methods of complex analysis appear to be very effective. This book presents methods of conformal mappings for analysis of motion of boundary surface at least in two-dimensional case. Thus, if $l_t \gg r$ the problem of crystallization of undercooled melt (1.1) – (1.3) and the problems considered above are formally equivalent and are typical representatives of the quasistationary Stefan problem. Making use of methods of complex variables allows us to reduce the problem discussed to a system of ordinary differential equations [8, 9, 10].

In this case problem (1.1) - (1.3) becomes one of the simplest among the ones considered above and is a kind of aquasistationary Stefan problem. However, even in this simple case, determination of the boundary is a rather complicated mathematical problem.

Reformulate now the problem (1.1) - (1.3) in terms of Laplacian growth problem. We investigate the growth of the two-dimensional region Q and suppose that its boundary is Γ , which represents the physical interface (Fig. 1). The field φ outside the region Q, satisfies the Laplace equation

$$(1.4) \Delta \varphi = 0.$$

The boundary Γ grows at a rate, that is proportional to the normal gradient of the field of the interface. Therefore the evolution of the interface is governed by the following equation

$$(1.5) v_n = -\nabla_{\mathbf{n}} \varphi|_{\Gamma}.$$

The potential field φ satisfies the following boundary condition on the interface

$$(1.6) \varphi|_{\Gamma} = d_0 k|_{\Gamma},$$

where k is the curvature of the interface Γ , and d_0 is the dimensionless surface tension parameter.

For this type of system the utilization of the theory of function of complex variable is very fruitful. Theoretical methods of the functions of complex variable appear to be rather useful in the construction of the effective surface dynamics of the interface at least in the two-dimensional problem. In this case the central issue of this problem belongs to the conformal mappings of the physical regions of the space onto some special kind of regions. A large number of models for interfacial dynamics had been proposed up to now. Reviews of these problems can be found in [11, 9, 12]. The most famous equation was introduced by Shraiman and Bensimon [14]. It is widely known as the conformal mapping equation and is still under investigation.

In examples of the quasistationary Stefan problem, the main point of its solution lies in construction of an appropriate potential specified by its boundary value. Physically it is possible to do only when the boundary of the domain of the potential is rather simple. The simplest examples of such region is a disk. If we know a conformal mapping of a disk on some region, the solution to the posed boundary problem reduces to change of variables in the solution for the disk. Thus, solution of the quasistationary Stefan problem for the two-dimensional region is practically reduced to determination of an appropriate conformal mapping or its equation of motion. It is possible to compare the non-stationary Stefan problem with an equivalent quasistationary Stefan problem. It allows us to solve a wider class of problems in framework of the equations of motion of the appropriate conformal mappings.

Let us consider the approach developed by Shraiman and Bensimon [9, 12, 14, 8, 16]. This approach is based on the Riemann mapping principle. This principle states the existence of a conformal map from the exterior of domain Q onto the standard domain, for example, the exterior of unit disk, with the boundary Γ corresponding to unit circle. In the outline under regard one can parametrize evolution of the interface in z plane by means of time-dependent conformal map F(w,t) which takes the exterior of the unit disk at each moment of time, $|w| \geq 1$, onto the exterior of Q. Therefore the evolution of the interface can be presented as follows:

(1.7)
$$\Gamma\left(\theta,t\right) = \lim_{w \to e^{i\theta}} F\left(w,t\right), \ 0 \le \theta < 2\pi.$$

As it is shown by Shraiman and Bensimon [14], in the case of free surface tension $(d_0 = 0)$ the boundary map satisfies the following equation of motion

(1.8)
$$\frac{\partial \Gamma(\theta, t)}{\partial t} = -i \frac{\partial \Gamma(\theta, t)}{\partial \theta} S \left[\left| \frac{\partial \Gamma(\theta, t)}{\partial \theta} \right|^{-2} \right] \bigg|_{w=e^{i\theta}},$$

where $S[\cdot]$ means the Schwartz operator [13]. For the exterior of a unit circle with some boundary condition $f(\theta)$ the Schwartz operator can be presented as follows:

(1.9)
$$S\left[f\left(\theta\right)\right] = -\frac{1}{2\pi} \int_{0}^{2\pi} d\theta' \frac{e^{i\theta'} + w}{e^{i\theta'} - w} f\left(\theta'\right) + iC,$$

where C is an arbitrary constant.

It was shown[15] that equation (1.8) is equivalent to equation of motion of certain field $\eta(\theta, t) = \left| \frac{\partial \Gamma(\theta, t)}{\partial \theta} \right|$:

$$\frac{\partial \eta(\theta,t)}{\partial t} = \frac{1}{R(t)} \frac{\partial \eta(\theta,t)}{\partial \theta} \frac{1}{2\pi} \int_{0}^{2\pi} d\theta' v_{n}(\theta',t) \eta(\theta',t) \cot \frac{\theta'-\theta}{2} - \frac{\eta(\theta,t)}{R(t)} \left[\eta(\theta,t) v_{n}(\theta,t) - \frac{1}{2\pi} \int_{0}^{2\pi} \eta(\theta',t) v_{n}(\theta',t) d\theta' \right] + \frac{\eta^{2}(\theta,t) v_{n}(\theta,t)}{R(t)} \frac{\partial}{\partial \theta} \frac{1}{2\pi} \int_{0}^{2\pi} d\theta' \ln \eta(\theta',t) \cot \frac{\theta'-\theta}{2} - \frac{\eta(\theta,t)}{R(t)} \frac{\partial}{\partial \theta} \frac{1}{2\pi} \int_{0}^{2\pi} d\theta' v_{n}(\theta',t) \eta(\theta',t) \cot \frac{\theta'-\theta}{2}$$
(1.10)

considered in [12, 16, 17]. Here the radius R and normal velocity v_n satisfy to the next equations:

(1.11)
$$\frac{dR}{dt} = \frac{1}{2\pi} \int_{0}^{2\pi} d\theta' \eta(\theta', t) v_{n}(\theta', t).$$

$$v_{n}(\theta, \eta, t) = \beta(\theta) \frac{\eta(\theta, t)}{R(t)} \left\{ \varphi_{0} - \frac{\psi_{s}}{R(t)} \frac{\partial}{\partial \theta} \frac{1}{2\pi} \int_{0}^{2\pi} d\theta' \cot \times \frac{\theta' - \theta}{2} \eta(\theta', t) d_{0}(\theta', \eta) \frac{\partial}{\partial \theta'} \left[\frac{1}{2\pi} \int_{0}^{2\pi} d\theta'' \cot \frac{\theta'' - \theta'}{2} \ln \eta(\theta'', t) \right] + \frac{\varphi_{s}}{R(t)} \frac{\partial}{\partial \theta} \frac{1}{2\pi} \int_{0}^{2\pi} d\theta' \cot \frac{\theta'' - \theta}{2} \eta(\theta', t) d_{0}(\theta', \eta) \right\}.$$

$$(1.12)$$

In local approximation last relationship has the form [12, 16, 17]:

(1.13)
$$v_n(\theta, \eta, t) = \frac{\eta(\theta, t)}{R(t)} \left(1 - \frac{1}{R(t)} \frac{\partial^2 \eta}{\partial \theta^2} \right).$$

The equations (1.10),(1.11),(1.13) are one-dimensional equations determined on the interval $[0,2\pi]$.

Now let us consider the linear stage of stability of a cylindrical boundary. In this case it is natural to put $d_0\left(\theta,\eta\right)=d_0=const, \beta\left(\theta,\eta\right)=\beta_0=const$. Linearizing equations (1.10), (1.11), (1.13) with respect to perturbations $\delta\eta=\delta\eta_0\exp(\int\limits_0^t\gamma\left(t'\right)dt'+ik\theta)$ at $k=\pm1,\pm2,...$ and taking into account the relation

$$\frac{1}{2\pi} \int_{0}^{2\pi} d\theta' \cot \frac{\theta' - \theta}{2} e^{ik\theta'} = i e^{ik\theta} \operatorname{sign} k$$

we obtain the following characteristic equation

(1.14)
$$\gamma = \frac{\beta}{R} \left[k - 2 + \frac{d_0}{R} k^2 (1 - k) \right].$$

It can be seen from equation (1.14) that the instability is realized for rather short-wave fluctuations with k > 2 [5]. At $d_0 \neq 0$ the fluctuations with wave number

(1.15)
$$k_0 = \frac{1}{3} \left(\sqrt{1 + 3 \left(\frac{d_0 \varphi_s}{R \varphi_0} \right)^{-1}} - 1 \right)$$

have the maximum increment of increase. The instability as $d_0 \to 0$ is observed within a wide spectrum of wave vectors, which causes complicated fractal structure of dendritic formations. The surface energy damps the instability subject to chosen wave vectors and gives rise to the minimum radius of curvature of a dendrite.

2. Numerical simulation of the interface dynamics

In the present section numerical simulation of the surface dynamics is given. We consider the properties of the interface dynamics from the viewpoint of singular integral equations.

2.1. Properties of the interface dynamics. Equations (1.10) and (1.11) are not directly related to the physical mechanism determining motion of the interface in real space. They determine the variation law governing the mapping of a circle into the contour Γ under the given normal velocity v_n . In framework of this approach we consider properties of equations (1.10), (1.11).

We will investigate the periodical structure formation, supposing that the structure will have period $2\pi/k$, where k is an integer. This make it possible to consider the solution only on the interval $[0, 2\pi/k]$. In fact, we shall consider some integrable periodic function

(2.1)
$$\widetilde{f}(\theta + n2\pi/k) = \widetilde{f}(\theta)$$

In this case the any singular integrals J in the equation (1.10) will look like:

$$(2.2) \frac{1}{2\pi} \int_{0}^{2\pi} d\theta' \widetilde{f}(\theta') \cot \frac{\theta' - \theta}{2} = \sum_{n=0}^{k-1} \int_{0}^{2\pi/k} d\theta' \widetilde{f}(\theta') \left(\cot \frac{\theta' + n2\pi/k - \theta}{2}\right) =$$

$$= \int_{0}^{2\pi/k} d\theta' \widetilde{f}(\theta') \Re(\theta' - \theta) du'$$

where

$$\Re(u'-u) = \sum_{n=0}^{k-1} \cot \frac{\theta' + n2\pi/k - \theta}{2}.$$

So, we can use for computer simulation the interval $[0,2\pi/k]$.

2.2. Numerical solution of the interface dynamics. The derived systems of nonlinear integro-differential equations were investigated numerically. The numeric simulation was based on approximation of unknown functions by trigonometrical polynomials. Expansions of this type make it possible to use well-known quadrature formulae to evaluate singular integrals. As a result, the system of equations (1.10), (1.11) and (1.13) reduces to a system of ordinary non-linear differential equations with filled Jacobian.

During computing experiments the approach based on approximations of searched functions by trigonometrical polynomials [18, 19]

(2.4)
$$\widetilde{f}_n(u) = \frac{1}{2\pi} \sum_{j=0}^{2n-1} \widetilde{f}(u_j) \sin[n(u-u_j)] \cot \frac{u-u_j}{2}$$

with the given nodes set

(2.5)
$$u_j = \frac{\pi j}{n}, \qquad j = 0, 1, ..., 2n - 1.$$

was used. The representation of the function $\tilde{f}(u)$ in form (2.4) makes it possible to apply the obtained analytical expressions practically for all derivatives of the function \tilde{f} during calculations.

Besides, expansion of the function $\widetilde{f}(u)$ into a trigonometrical polynomial makes it possible to use quadrature formulae [18, 19] for calculation of singular integrals with Hilbert kernels, that is

(2.6)
$$J(u_m^0) = \sum_{j=0}^{2n-1} \frac{1}{2n} \widetilde{f}(u_j) \cot \frac{u_j - u_m^0}{2}$$

being defined on the system of nodes

(2.7)
$$u_m^0 = \frac{2\pi m + 1}{2\pi}, \qquad m = 0, 1, ..., 2n - 1.$$

Taking now into account that all integrand functions on the right hand side of equations (1.10), (1.12) are of the same kind it is possible to present them in the form of (2.6) making the following assignments

(2.8)
$$\eta_m(t,u) = \eta(t,u_m^0), \qquad m = 0,1,...,2n-1.$$

As a result from the equations of interface dynamics we obtain the system of ordinary differential equations:

(2.9)
$$\frac{d\eta_m}{dt} = \widehat{F}_m \left\{ \left\{ \eta_m, \sum_{j=0}^{2n-1} f_j \cot \frac{u_j - u_m^0}{2} \right\}, \right.$$

where $\widehat{F_m}$ is a nonlinear operator being determined by the right hand side of equations (1.10), (1.11) (1.12), f_j can take values $v_n(u_j)\eta(u_j)$, $\ln \eta(u_j)$, $\eta(u_j)$ and etc.

Numerical integration of specified systems was carried by means of discrete calculation of the Jacobian when realizing implicit methods of Girr and Adams

FIGURE 2. Non-uniform distribution of the $\eta(\theta, t), \psi(\theta, t)$ and the corresponding interfaces for the following initial perturbation: $\eta(\theta, t_0 = 0) = 1.0 - 0.01 \cos(4\theta); d_0 = 0.05$; interfaces on the figure correspond to the time steps $(t_{step} = 0.5*10^4)$ 18 times are plotted, spaced between $0 < t \le 0.8*10^4$.

[20]. Choice of the value of discretization and the local error of integration was made so that the necessary accuracy of the searched solution and the stability of calculations were ensured. Making use of variable $\eta\left(u_{m}^{0}\right)$ changing in time, subject to the transformations

(2.10)
$$dy = \frac{R(t)d\theta}{\eta(\theta,t)}\sin\left(\theta + \psi(\theta) + \frac{\pi}{2}\right),$$
$$dx = \frac{R(t)d\theta}{\eta(\theta,t)}\cos\left(\theta + \psi(\theta) + \frac{\pi}{2}\right)$$

for the system of equations (1.10), (1.11) and (1.13) it is possible to reproduce geometrically defined interfaces in parametric form.

In this text we evidently do not claim the complete investigation of pattern formation in free boundary problems. Our goal is to show that developed approach can be applied to investigation of interface evolution. Results of computer simulation presented below give rise only to some sketch of the structures realizing in the systems under consideration.

During numerical simulation evolution of the interface was investigated. The product term β affect only on time scale of the process. Therefore, in the analysis under regard $\beta=1$ is taken. It was found out that the surface energy influences the behavior of the field $\eta\left(\theta,t\right)$ and interfaces too much. At small values of the surface energy rather small-sized structures can be formed. As d_0 increases the structures take a more smooth form.

Figure 2 illustrates the characteristic form of non-uniform distributions of the field η (plot a) and the corresponding interfaces (plot b).

It is possible to observe that relatively smooth variations of the interface correspond to rather great variations in the field η as well as in the angle ψ . Thus, relatively small errors in determining η do not cause great changes in the interface geometry. In addition, as is seen from Figures 2 relatively even long sections of the interface shrink when mapped onto the interval $[0,2\pi]$, whereas sharp changes in the contour Γ , conversely, are stretched out. In this sense such mappings are

FIGURE 3. Comparison of interface profiles for different values of surface tention d_0 : $d_0=0.15-a$); $d_0=0.12-b$); $d_0=0.09-c$); $d_0=0.06-d$); $d_0=0.04-e$); $d_0=0.03-f$). Initial perturbations for all the figures are the same: $\eta(\theta,t_0=0)=1.0-0.01\cos(4\theta)$; $(t_{step}=0.5*10^4)$ 18 times are plotted, spaced between $0 < t \le 0.8*10^4$.

"adaptive" with respect to the information about the detailed geometric structure of the interface.

The characteristic geometry of the structures obtained as a result of computer simulation of a small perturbation is presented on Figures 3, and 4. The smaller capillary length is the more diverse structure arises. Figures 3, and 4 are different from each other due to periodicity of the initial perturbation.

If the system is influenced by an uncorrelated noise with the normal law of distribution unregular structures arise. During simulation it was taken that on each step of integration the velocity at point i of the interval $[0, 2\pi]$ equal to $v_n(\theta_i) + (\eta/R)^{1/2} \delta v_n(\theta_i)$, within $\delta v_n(\theta_i)$ being chosen in the correspondence with the normal law of distribution in limits $(-10^{-5}, 10^{-5})$ (Fig. 5).

For simulation of anisotropic growth of crystals the following expression (similar as in [21]) was used:

$$(2.11) d_0(\theta) = (1 - 15\gamma_4 \cos 4\gamma)d_0 =$$

$$= \left[1 - 15\gamma_4 \cos 4\left(\theta - \frac{1}{2\pi} \int_0^{2\pi} d\theta' \ln \eta(\theta') \cot \frac{\theta' - \theta}{2}\right)\right] d_0.$$

The interfaces corresponding to the capillary length (2.11), subject to the anisotropy of surface energy have the form of truly looking cross (Fig. 6, and 7), despite that at the initial moment the boundary surface presents a circle (up to

FIGURE 4. Comparison of interface profiles for different values of surface tention d_0 : $d_0 = 0.15 - a$); $d_0 = 0.12$ -b); $d_0 = 0.09$ -c); $d_0 = 0.06$ -d); $d_0 = 0.04$ -e); $d_0 = 0.03$ -f). Initial perturbation for all the figures is the same: $\eta(\theta, t_0 = 0) = 1.0 - 0.01 \cos(6\theta)$; $(t_{step} = 0.5 * 10^4)$ 18 times are plotted, spaced between $0 < t \le 0.8 * 10^4$.

FIGURE 5. Interface dynamics stimulated by external noise.

 $\delta v_n|_{t=0} \cong 10^{-5}$). According to the value of γ_4 such an anisotropy is exhibited at small or large values of R and t. The realized distributions little depend on initial perturbations and reduce frequently to rather complicated and exotic surfaces. A more developed structure in the case of anisotropy is presented by Fig. 8. An example of structures arising from nonhomogeneous initial conditions is illustrated by Fig. 9, a). In the same time Fig. 9, b) illustrates an example of structures developing from a flat boundary.

It should be noted that at $d_0 = 0$ the results concerning smooth boundary under stochastic excitation of short-wave perturbations, caused for example by errors of calculations do not lead the developed structures due to instabilities of computation.

References

FIGURE 6. Non-uniform distribution of the $\eta(\theta,t), \psi(\theta,t)$ and the dendrite silhouette for surface tension anizotropy: $\eta(\theta,t_0=0)$. = $1-0.01\cos(4\theta); d_0=0.3; \ \gamma_4=0.05$ interfaces on the figure correspond to the time steps($t_{step}=0.25*10^4$) 15 times are plotted, spaced between $0 < t \le 0.325*10^5$.

FIGURE 7. Comparison of interface profiles for different values of surface tension anizotropy: $d_0 = 0.3$; a) γ_4 =0.00; b) γ_4 =0.01 c); γ_4 =0.02; d) γ_4 =0.04. Initial perturbation for all the figures is the same: $\eta(\theta, t_0 = 0) = 1. -0.01\cos(4\theta)$; $(t_{step} = 0.25 * 10^4)$ 15 times are plotted, spaced between $0 < t \le 0.325 * 10^5$.

^[1] Moving Boundaries VI Computational Modelling of Free and Moving Boundary Problems, Eds: B. Sarler, C.A. Brebbia, Series: Computational and Experimental Methods Vol: 4, WIT Press, (2001).

^[2] Free Boundary Problems: Theory and Applications Ed. by I. Athanasopoulos, (Chapman & Hall /CRC Research Notes in Mathematics, 409) Hardcover (1999).

^[3] E. Ben-Jacob , N. Goldenfeld , L. S.Langer, G. Schon, Dynamics of Interfacial Pattern formation. Phys. Rev. Lett., **51**, #21, p. 1930, (1983).

FIGURE 8. Dendrite silhoette for surface tension anizotropy: $\gamma = 0.03$, $d_0 = 0.03$, $\eta(\theta, t_0 = 0) = 1 - 0.01 \exp\left(\frac{\theta - \pi/4}{0.1}\right)^2$, $(t_{step} = 0.2 * 10^4)$ 21 times are plotted, spaced between $0 < t \le 0.36 * 10^4$.

FIGURE 9. Dendrite silhoette for surface tension anizotropy: $\gamma=0.00,\ d_0=0.03,\ \eta(\theta,t_0=0)=1-0.01\exp\left(\frac{\theta-\pi/4}{0.1}\right)^2,\ (t_{step}=0.1*10^4)\ 13$ times are plotted, spaced between $0< t\leqslant 0.12*10^4.-a)$. The evolution of the flat boundary with small initial perturbation $\eta\left(t=0\right)=1-0.01\cos u\ -b)$.

- [4] W. W. Mullins and R. F. Sekerka, Stability of a planar interface during solidification of a dilute binary alloy. J. Appl. Phys., 35, 444, (1964).
- [5] W. W. Mullins and R. F. Sekerka, Morphological stability of a Particle growing by diffusion or heat flow. J. Appl. Phys. v.34, 323, (1963).
- [6] E. Ben-Jacob , N. Goldenfeld, J. S.Langer, G. Schon, String models of interfacial pattern formation., Physica D., 12, #1/3, p. 245, (1984).
- [7] E.Ben-Jacob, N.Goldenfeld, J. S.Langer, G.Schon, Pattern selection in Dendritic Solidification. Ibid. 53, #22. p. 2110, (1984).
- [8] D. Bensimon Stability of viscous fingering, Phys. Rev. A, 33, #2, p.1302, (1986).
- [9] D.Bensimon, L.P.Kadanojf, S.Liana, B. J.Shraiman, Chao Tang, Viscous flows in two dimensions. Rev. of Modern Phys. 58, #4, p. 977, (1986).
- [10] D.Bensimon, P.Peice, Tip-splitting solutions to a Stefan problem. Phys. Rev., 33, #6, p. 4471, (1986).

- [11] Dynamics of Curved Fronts, ed. by P.Pecle, Academic Press, San Diego (1988).
- [12] V.V.Gafiychuk, I.A.Lubashevskii, V.V.Osipov. Dynamics of surface structures in systems with a free boundary. Naukova Dumka, Kiev, 1990. 214 pp. ISBN5-12-001274-4.
- [13] H. Begehr, R. Gilbert, Transformations, transmutations, and kernel functions, 1, Longman Publishers, Harlow, 399 pp., (1992).
- [14] A. Shraiman, D. Bensiman, Singularities in nonlocal interface dynamics, Phys. Rev. A., 30, # 5, 2840, (1984).
- [15] V.Gafiychuk, A.Shnyr, B.Datsko, Interface dynamics equations: their properties and computer simulation, http://xxx.lanl.gov/nlin.AO/0011021 (2000).
- [16] V.V.Gafiychuk, I.A.Lubashevskii. Non-local dynamics of dendritic growth. Zh. Khim. Fiz. (USSR) v.7, No.9, p.852 - 859 (1988) (in Russian).
- [17] V.V.Gafiychuk, I.A.Lubashevskii. Analysis of the dynamics of phase interfaces in a quasi-stationary Stefan problem. Zh. Vychisl. Mat. Mat. Fiz. (USSR) v.29, No.9, p.1331-1345 (1989) (English translation in Compute. Math. Math. Phys. (UK)).
- [18] S.M.Belozerkovsky, I.K.Lifanov, Numerical methods in the singular and integral equations. Nauka, (1985). (in Russian).
- [19] V.V.Panasyuk, M.P.Savruk, Z.T.Nazarchuk. Method of singular integral eguations in twodimensional diffraction problem. Naukova Dumka, Kiev, 1984 (in Russian).
- [20] Byrne J., Hindmarch D.C. Stiff ODE Solver: A review of Current and Coming Attractions // J. Comput. Phys.- 1987.-70, N l.-P. 1-60.
- [21] P.W. Vorhees, S.R. Coriell, G.A. McFadden, The effect of anisotropic crystal-melt surface Tension on grain boundary groove morphology, J. Cryst. Growth. 67, 425, (1984).

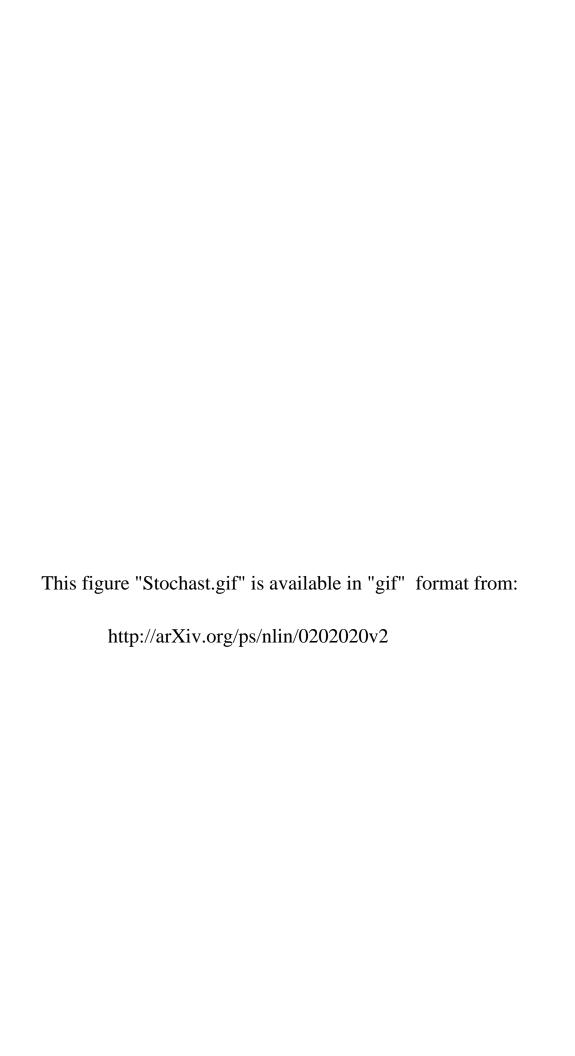
New Jersey Institute of Technology University Heights Newark, NJ 07102-1982 $E\text{-}mail\ address:}$ roandr@megahertz.njit.edu URL: http://eies.njit.edu/~andrushk/

Institute of Applied Problems of Mechanics and Mathematics, National Academy of Sciences of Ukraine, Lviv

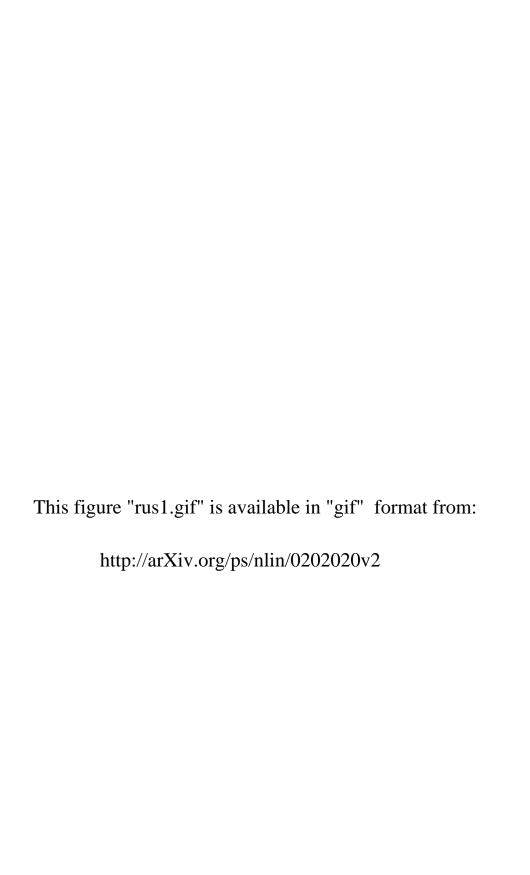
E-mail address: viva@iapmm.lviv.ua

Institute of Applied Problems of Mechanics and Mathematics, National Academy of Sciences of Ukraine, Lviv

 $E ext{-}mail\ address: viva@iapmm.lviv.ua}$

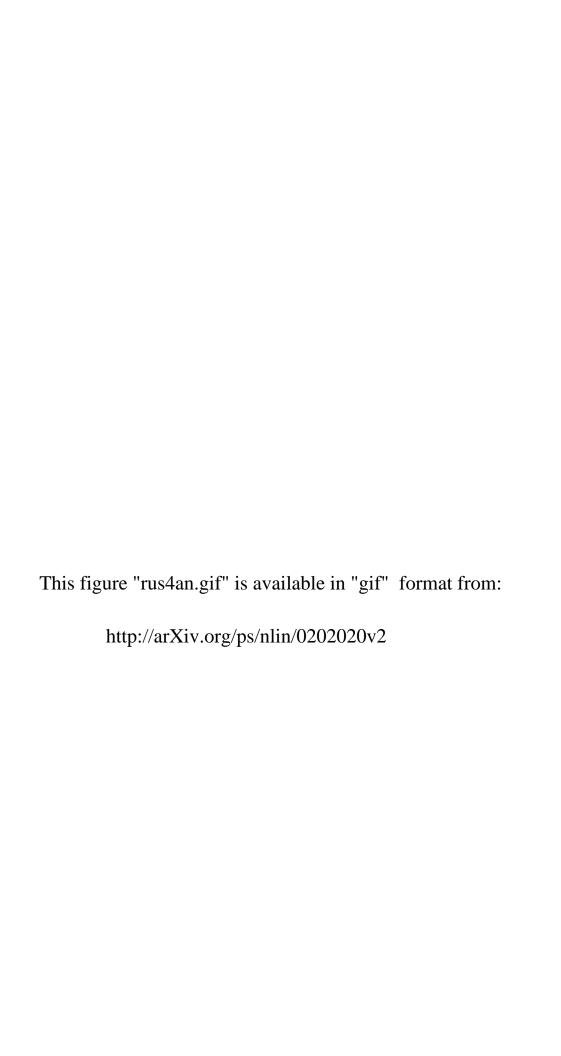


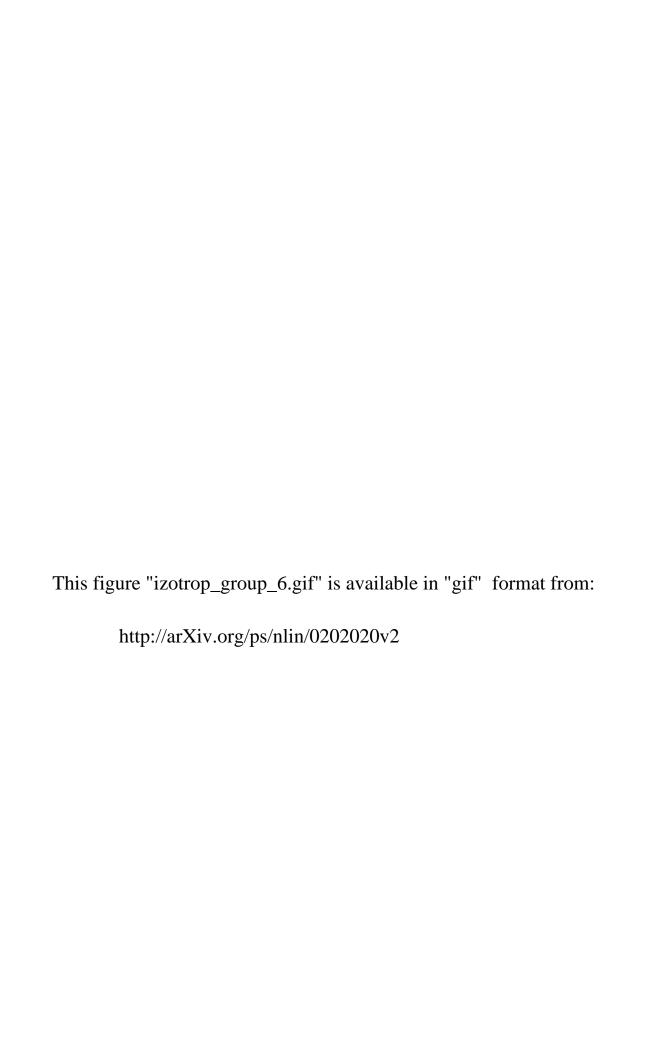




This figure "rus2.gif" is available in "gif" format from:

This figure "rus3.gif" is available in "gif" format from:





This figure "rus7.gif" is available in "gif" format from:

This figure "F11n.gif" is available in "gif" format from: